World Journal of Advanced Research and Reviews
eISSN: 2581-9615 CODEN (USA): WJARAI
Cross Ref DOI: 10.30574/wjarr
Journal homepage: https://wjarr.com/

(RESEARCH ARTICLE)

Check for updates

Strategy for optimizing geophysical deployment: Case study of an HVA drilling project in the Kong bedrock environment

Bouadou [1,*], Rock Armand Michel, Coulibaly [2], Adama, Kouassi [1], Kouamé Auguste and Gnagne Théophile [1]

[1] *UFR of Sciences and Management of the Environment, University of Nangui Abrogoua, Abidjan, Côte d'Ivoire*
[2] *UFR of Earth Sciences and Mineral Resources, University of Félix Houphouët-Boigny Abidjan, Côte d'Ivoire*

World Journal of Advanced Research and Reviews, 2025, 28(01), 186-200

Publication history: Received on 21 August 2025; revised on 01 October 2025; accepted on 04 October 2025

Article DOI: https://doi.org/10.30574/wjarr.2025.28.1.3425

Abstract

This study aims to develop a strategy for optimizing the selection of geophysical sites for HVA drilling in the bedrock area of Kong. To achieve this objective, the methodology first consisted of extracting the fracture network from satellite image processing. Then, surveys and electrical drags were used to characterize the geometry of the fractured aquifers (the depths of the aquifer zones and the fracturing indices of the conductive anomalies). The conductive anomalies K, H, U, and V were identified by electrical drags and intersected the fractures determined by processing Landsat 7 ETM+ satellite images. In addition, the fracturing index ranges from 1.96 to 2.57. The corrected cumulative lengths of the fractures range from 362.92 m to 835.46 m. Interpretation of the borehole curves showed 4 to 5 aquifer zones in the subsoil. Finally, combining the fracturing index, the depth of the aquifer zones, and the length of the fractures resulted in the following drilling priority order: K (F1), U (F2), V (F3), and H (F4) (K > U > V > H).

Keywords: Geophysical Survey; Electrical Resistivity; Fracture Length; Bedrock Aquifer; Kong; Côte d'Ivoire

1. Introduction

To manage and prevent crises related to access to water, the theme for World Water Day (WWD) 2022 is "Groundwater: Making the Invisible Visible." This is because almost all of the planet's freshwater reserves are underground, serving to supply drinking water, sanitation systems, agriculture, industry, and ecosystems. Therefore, to make groundwater (the invisible) visible, indirect methods of exploring the subsoil are used to identify this natural resource before drilling. However, the question is how much is needed to supply populations, industries, and other economic and social activities in the long term. In this context, geophysics [1], remote sensing [2] and geomorphology [3] are methods used to indirectly locate groundwater aquifers. However, the choice of location remains crucial, as the chosen site must be able to produce the amount of water needed to meet expected long-term needs. With this in mind, this study seeks to develop a strategy aimed at optimizing the choice of geophysical sites for HVA-type drilling in order to meet the water needs required to satisfy certain human requirements.

2. General information about the study area

2.1. Presentation of the study environment

The project site is located approximately 4 km southwest of the city of Kong. Located at longitudes 4°38'01" and 4°37'38.6" West and latitudes 9°07'04.4" and 9°07'26.9" North, the study area is part of the Tchologo region, whose regional capital is the town of Ferkessedougou. The vegetation is of the tree and shrub savanna type and is severely degraded. The area is drained by the Comoé River. Annual rainfall over the past three decades has varied between 800 and 1,500 mm, with an average of 1,300 mm [4].

* Corresponding author: Rock Armand Michel BOUADOU

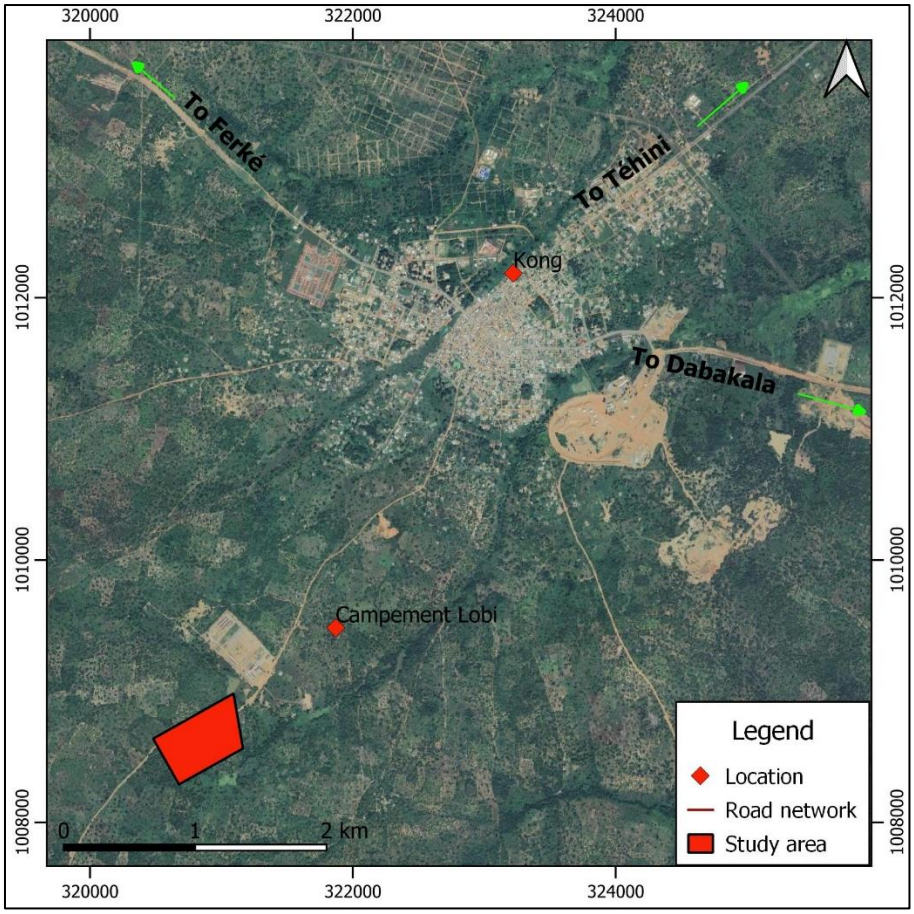

Figure 1 Geographic location of the study area

2.2. Hydrogeological and geological context

Geologically, the site under study is located in an area of crystalline and crystallophyllian rocks. The geological formations in the region rarely outcrop because they are covered by a thick layer of weathered rock. However, the geological map indicates that the project site is located on heterogeneous biotite granitoid formations [3] (Figure 2). From a hydrogeological point of view, the aquifer system in the study area therefore consists of a (superficial) weathered rock aquifer, beneath which lies the fissure and fracture aquifer.

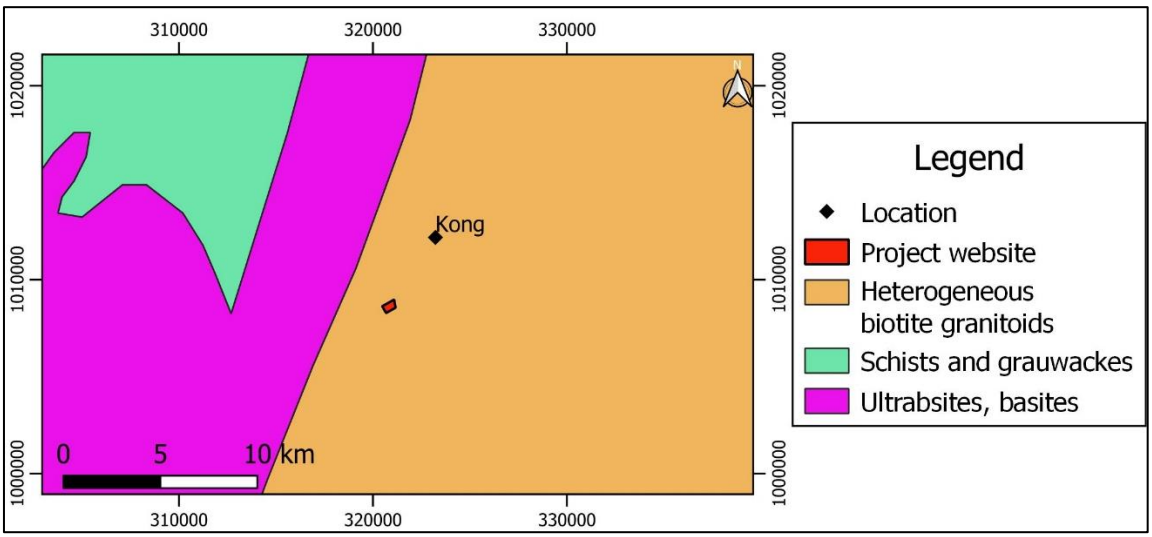

Figure 2 Geological map of the study area

3. Material and methods

3.1. Geophysical prospecting equipment

The measuring equipment used is a Syscal R2 resistivity meter from Iris Instruments (Figure 3). It can be used to perform both electrical dragging and electrical sounding. However, its use for geophysical prospecting requires a number of useful devices and accessories, such as:

- a 12-volt external battery to supply electrical power;
- an amplifier to increase the voltage of the electrical signal from the 12-volt battery to 200 volts, or even 400 to 800 volts;
- stainless steel electrodes are implanted in the ground to inject the amplified electrical current;
- four (4) reels of electrical cable, including two (2) 200-meter reels and two (2) 400-meter reels. These connect the resistivity meter to the electrodes;
- a compass for orienting the electrical drags;
- A GPS device is used to record the coordinates (longitude, latitude, and altitude) of each cable and survey carried out.
- Clamps are used to connect the electrical cables to the stainless steel electrodes driven into the ground.
- Two 100 m measuring tapes are used to position the electrodes at the selected measurement interval.
- Hammers are used to drive the electrodes into the ground.

Figure 3 Electrical resistivity measurement equipment: a) a Syscal R2 and an electrical current amplifier, and b) four electrical cable coils, a hammer, and electrodes

3.2. Methods

3.2.1. Lineament extraction study

The lineament extraction method is presented below. Landsat 7 image contour enhancement to improve image contrast [5]. Band ratios were used to improve the perception of the Landsat 7 image. The band ratios used are: ETM+4/ETM+5; ETM+4/ETM+6; ETM+7/ETM+6; ETM+5/ETM+4; (ETM+7-ETM+4) / (ETM+7+ETM+4); (ETM+6–ETM+4) / (ETM+6 + ETM+4). Finally, the Sobel filter, the Prewitt gradient filter, and the gradient filter developed by [6] were used to highlight the boundaries between two landscapes or specific features of the image such as lineaments, roads, etc. (Table 1).

Table 1 7 × 7 matrices of Sobel and gradient filters

N-S direction Sobel filter							E-W direction Sobel filter						
1	2	3	4	3	2	1	1	2	3	0	-3	-2	-1
2	3	4	5	4	3	2	2	3	4	0	-4	-3	-2
3	4	5	6	5	4	3	3	4	5	0	-5	-4	-3
0	0	0	0	0	0	0	4	5	6	0	-6	-5	-4
-3	-4	-5	-6	-5	-4	-3	3	4	5	0	-5	-4	-3
-2	-3	-4	-5	-4	-3	-2	2	3	4	0	-4	-3	-2
-1	-2	-3	-4	-3	-2	-1	1	2	3	0	-3	-2	-1
NE-SO direction Sobel filter							NO-SE direction Sobel filter						
0	1	2	2	3	3	4	4	3	3	2	2	1	0
-1	0	3	4	4	5	3	3	5	4	4	3	0	-1
-2	-3	0	5	6	4	3	3	4	6	5	0	-3	-2
-2	-4	-5	0	5	4	2	2	4	5	0	-5	-4	-2
-3	-4	-6	-5	0	3	2	2	3	0	-5	-6	-4	-3
-3	-5	-4	-4	-3	0	1	1	0	-3	-4	-4	-5	-3
-4	-3	-3	-2	-2	-1	0	0	-1	-2	-2	-3	-3	-4
Prewitt gradient filter							[6] gradient filter						
1	1	1	1	1	1	1	1	1	1	1	1	1	1
1	1	1	1	1	1	1	1	1	1	1	1	1	1
1	1	1	1	1	1	1	1	1	1	1	1	1	1
-1	-2	-3	-7	1	1	1	0	0	0	0	0	0	-1
-1	-2	-3	-3	1	1	1	-1	-1	-1	-1	-1	-1	-1
-1	-2	-2	-2	1	1	1	-1	-1	-1	-1	-1	-1	-1
-1	-1	-1	-1	1	1	1	-1	-1	-1	-1	-1	-1	-1

Using images generated from the processing and criteria defining image discontinuities, a map of visible linear structures was produced. Image discontinuities corresponding to presumed structural lineaments were identified manually following visual analysis on screen.

3.2.2. Geophysical study: Implementation of the electrical resistivity method

The electrical resistivity method, which is well suited to groundwater prospecting in crystalline bedrock areas, was used to explore the selected sites. The method was implemented using lateral investigation devices (electrical drags) and vertical investigation devices (electrical soundings).

The main drag and its parallels make it possible to highlight the fracture axes [7]. At points along these axes that show interesting signs, the vertical investigation method makes it possible to determine, vertically from these points, the succession of soil layers crossed by the electric current injected into the subsoil.

The Gradient Rectangle device is the lateral investigation device chosen for all surveys with a 600 to 800 m current injection line. For electrical surveys, the Schlumberger device is used with a 300 m current injection line (AB).

3.2.3. Study of the fracturing index

Based on an electrical profile, conductive anomaly shapes are well defined. They are essential in choosing electrical sounding points in the basement zone [8]. Depending on the shapes of these anomalies, attention is focused on two

parameters: the width (L) and amplitude (H) of the observed conductive anomalies (Figure 4). These two (2) parameters were used to define the fracturing index (IF) using the following equation:

$$IF = \frac{H}{L \times \rho_{amin}} \times 100$$

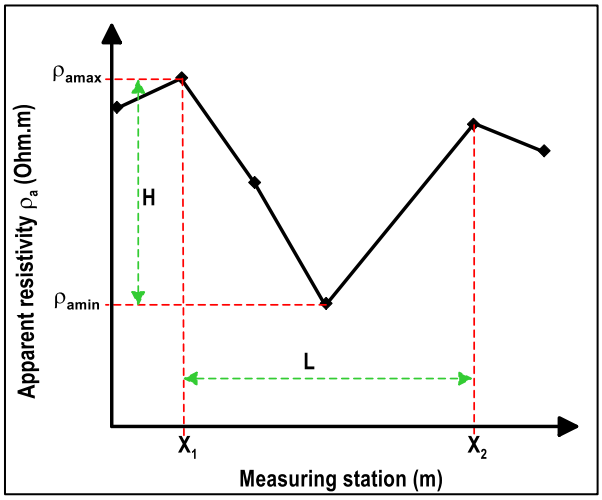

Figure 4 Calculation model for the fracturing index (IF)

The fracturing index is a parameter that provides information on the degree of fracturing in a rock.

3.2.4. Correction of cumulative fracture lengths

Considering an electrical sounding point located in a fracture network, it will intersect fractures of various lengths and directions that will have varying contributions to the productivity of future drilling. Fractures in the same direction as the main fracture will contribute more to the productivity of the capture structure than fractures in opposite directions. This is because the change in direction induces singular and linear pressure losses related to the lengths and intersections of these fractures.

This is why, in order to determine the cumulative length of fractures directly above or as close as possible to the electrical survey points, correction coefficients have been applied to each gross length to give a corrected length. This correction coefficient is the cosine of the angle between the intersecting fracture or the closest possible fracture and the neighboring fracture (Figure 5).

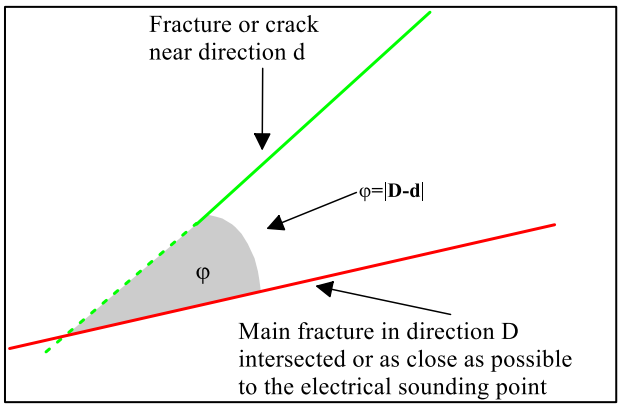

Figure 5 Diagram showing the fracture intersecting or as close as possible to the electrical sounding point and the neighboring fracture

The correction was performed using the following formulas:

$$L_c = L \times \cos(\varphi)$$

$$L_{cc} = \sum L_{c_n}$$

With

- L_c : the corrected length (m);
- L : fracture length (m);
- φ : difference between the neighboring direction (d) and the direction of the intersecting fracture or the closest possible direction (D) (φ=|D-d|);
- L_{cc}: the cumulative corrected length of the fractures (m);
- n : the number of fractures.

4. Results

4.1. Map of lineaments

The figure shows a detailed map of 65 lineaments identified on Landsat 7 ETM+ images of the study area. The lineaments range in length from 1.31 km to 9.97 km, with an average length of 3.67 km and a standard deviation of 2.04 km.

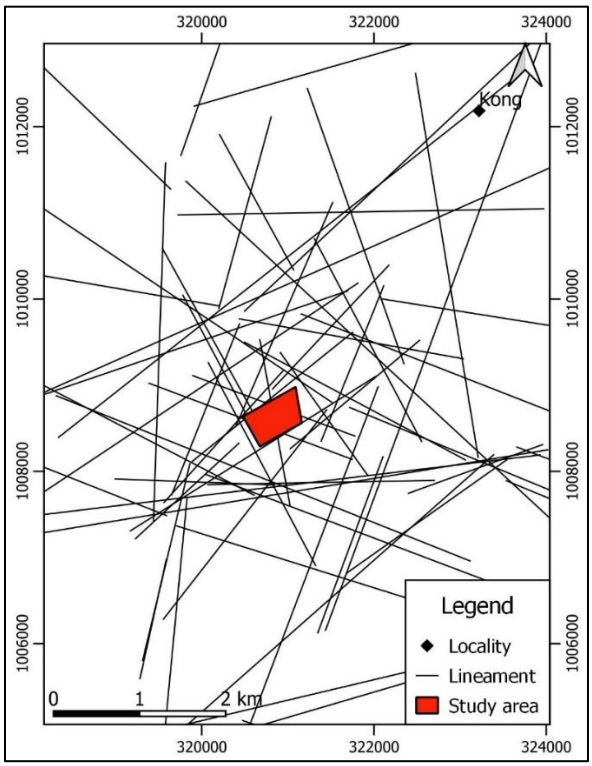

Figure 6 Detailed map of the lineaments in the study area

4.2. Validation of the lineament map

Drilling carried out by geophysicists in the study area has enabled the lineament map to be validated. The flow rate of these boreholes is between 7 and 15 m3/h. These boreholes, located on or near the lineaments, confirm that these catchment structures intersect fractures detected by geophysicists (Figure 6). Consequently, the relationship between productive boreholes and lineaments confirms the existence of fractures that are likely to constitute groundwater aquifers.

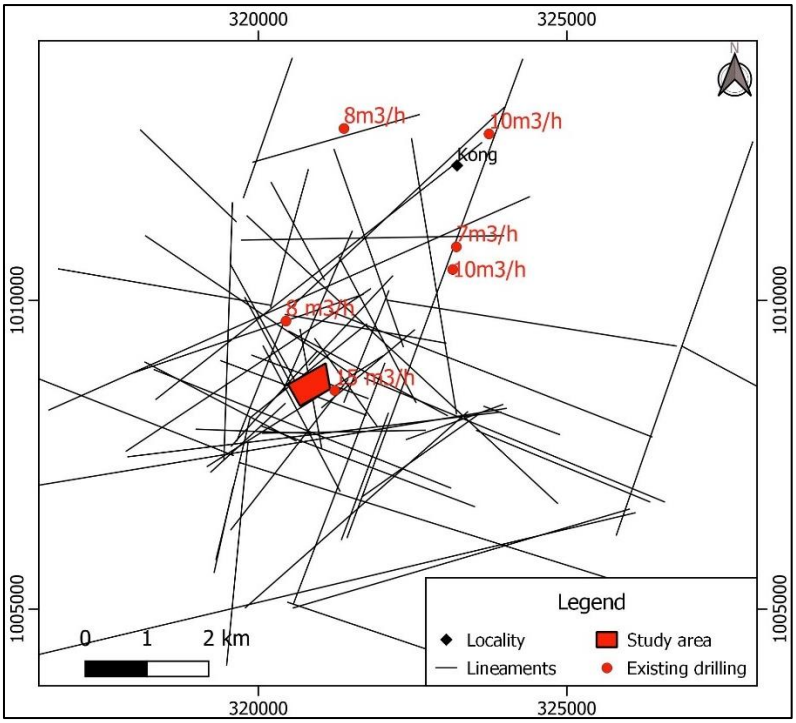

Figure 7 Superimposition of existing boreholes on the lineament map

4.3. Directional fracture rosette and choice of orientation for electrical logging

The directional rosette shows 18 direction classes with an angular increment of ten degrees (10°). The directional rosette shows an uneven distribution across the 18 classes, with direction family frequencies ranging from 0% (N170-180°) to 12.31% (N110-120°) (Figure 8). This diagram shows that the N110-120° (NW-SE) azimuth classes are the most common with 12.31%, followed by the N10-20° (N-S), N40-50° (NE-SW), N100-110° (NW-SE), and N150-160° (NWW-SEE). These secondary fracture direction classes have respective proportions of 10.77%, 9.23%, 9.23%, and 9.23%.

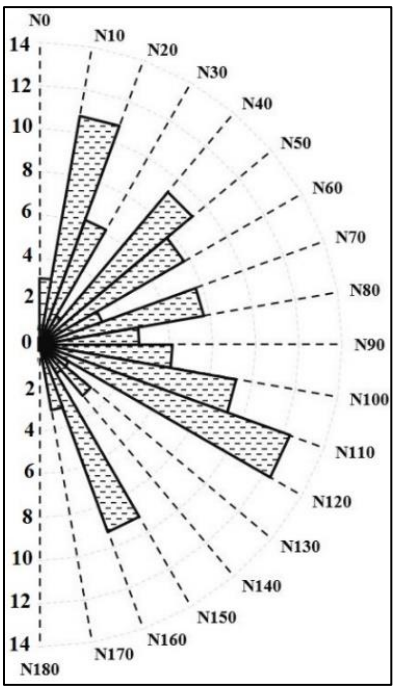

Figure 8 Directional rosette of fractures

In order to intersect fractures from the main NW-SE, N-S, NE-SW, and NWW-SEE direction classes, the electrical survey lines were laid out in an east-west (E-W) or west-east (W-E) orientation.

4.4. Selection of conductive anomalies based on the fracture map

After identifying the direction of the electrical profiles, one main electrical trench L0_0+00 and two (2) others L0_0+54 South and L0_1+00 North parallel to the main one were dug in the N°90 direction, each covering a distance of 390 m. Four conductive anomalies coincided with fractures identified from satellite image processing (Figure 9). These conductive anomalies were therefore selected for vertical prospecting of the subsoil in the study area.

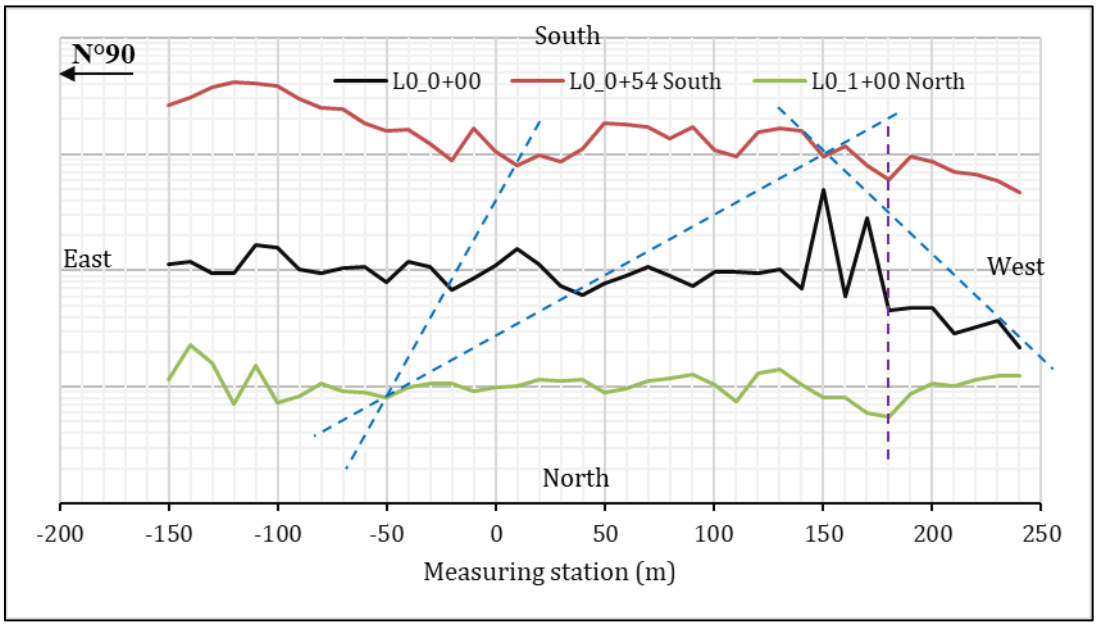

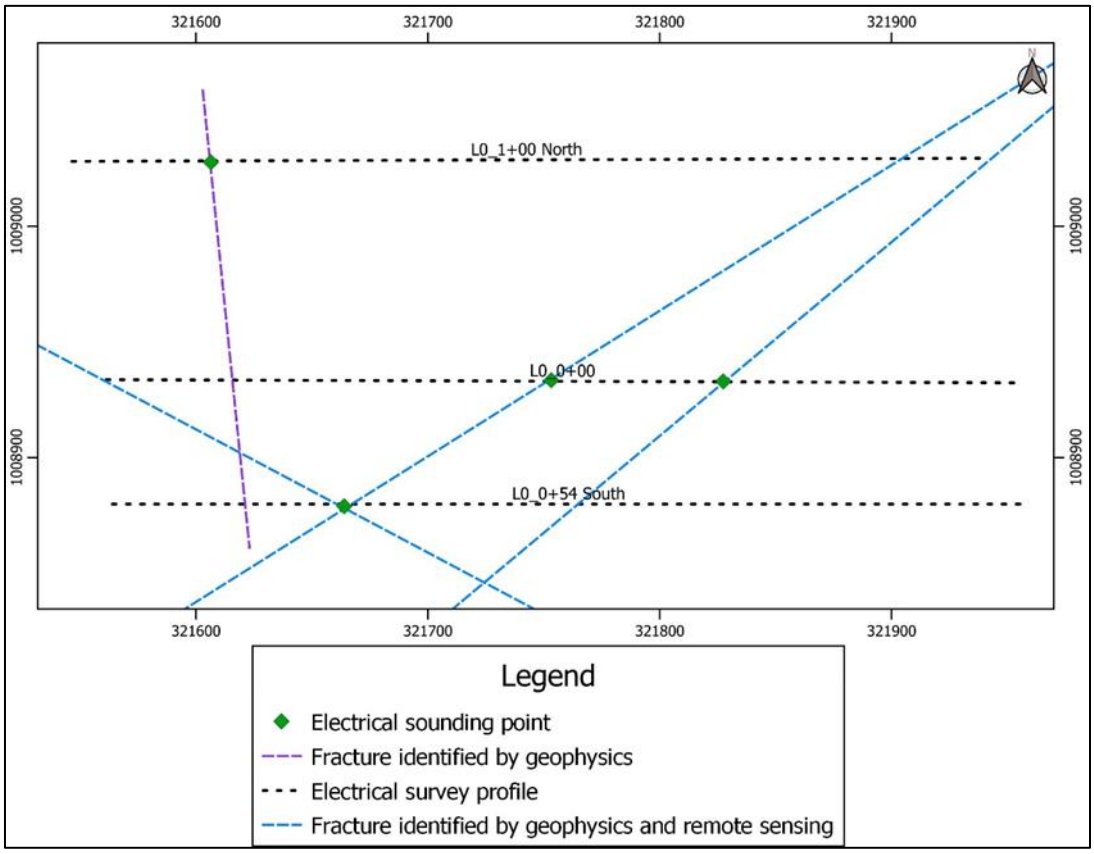

Figure 9 Superimposition of electrical profiles on the fracture map

4.5. Shape of conductive anomalies and their fracture indices

Four different shapes of conductive anomalies were identified (Figure 10). On profile L0_0+00, "V"-type and "U"-type conductive anomalies were identified at measuring stations -20 m and +40 m, respectively. K-type and H-type conductive anomaly shapes were also observed at the +140 m measuring station on the L0_0+54 South profile and at the +180 m measuring station on the L0_1+00 North profile, respectively.

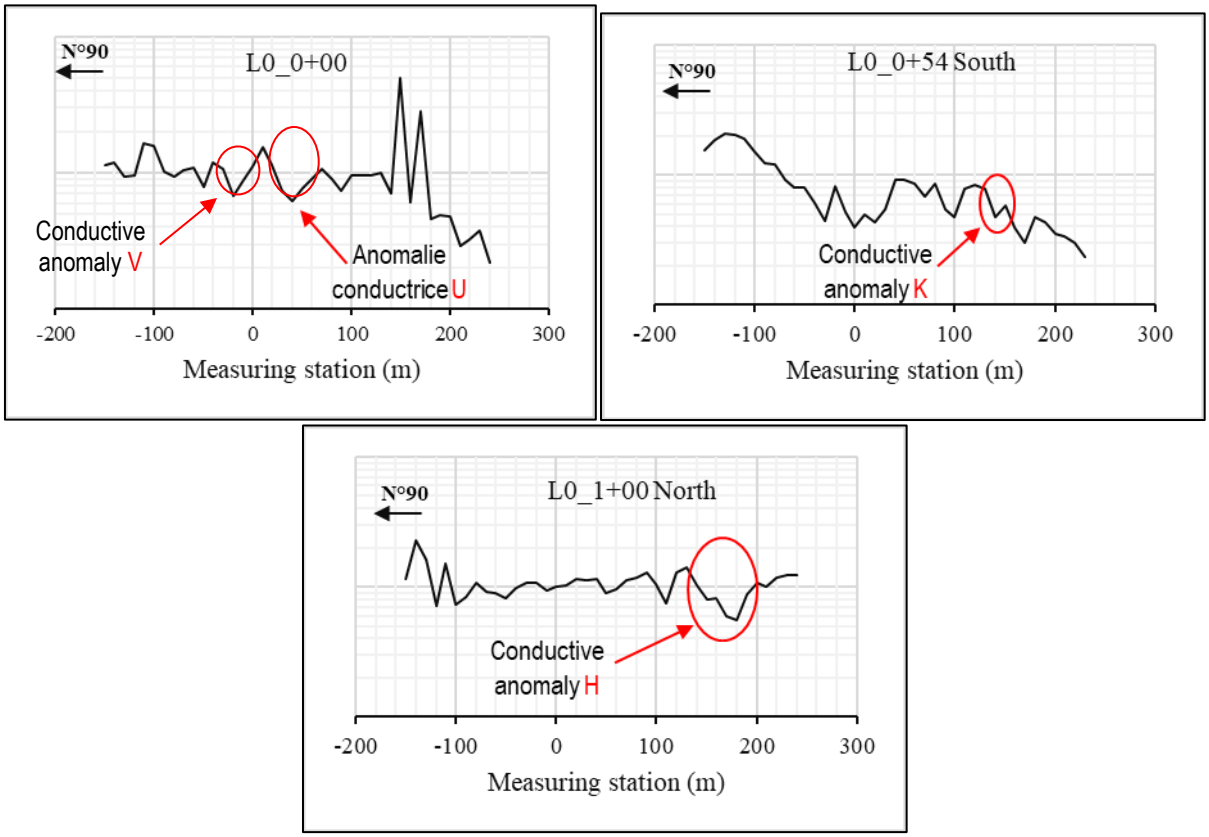

Figure 10 Graph showing conductive anomalies identified on electrical profiles

Table 2 shows that fracture indices vary from one type of conductive anomaly to another, with values ranging from IF = 1.96 (type "H" anomaly) to IF = 2.57 (type "K" anomaly).

Table 2 Fracturing index for types of conductive anomalies

Conductive anomaly	Electric drag line	Width L (m)	Amplitude H (Ohm.m)	Minimum apparent resistivity (Ohm.m)	Fracture index (IF)
V	L0_0+00	50	862	677	2.55
U	L0_0+00	60	916	623	2.45
K	L0_0+54 South	30	365	473	2.57
H	L0_1+00 North	30	326	554	1.96

The "V" type anomaly has a width of 50 m, an amplitude of 862 Ohm.m, and a fracturing index of 2.55. Next, the "U" type conductive anomaly has a width of 60 m, an amplitude of 916 Ohm.m, and a fracturing index of 2.45. As for the "K" anomaly, a width of 30 m, an amplitude of 365 Ohm.m and a fracturing index of 2.57 were determined. Finally, the "H" anomaly had a fracture index of 1.96, a width of 30 m, and an amplitude of 326 Ohm.m.

It should be noted that the higher the fracturing index value, the more important the anomaly is as a choice for the electrical sounding site. Thus, in order of priority, the order of importance of the types of conductive anomalies is as follows: K, V, U, and H (K > V > U > H).

4.6. Analysis of electrical sounding curves

After analyzing the lineament map and fracture index studies, electrical surveys were conducted directly above four (04) selected conductive anomalies. The electrical surveys carried out have increased hydrogeological significance. The survey curves recorded are all of the "KH" type. They are composed of four (4) clearly distinguishable electrical terrains (Appendix).

- The first electrical terrain is a surface layer corresponding to a more or less conductive sandy Arab soil cover.
- The second terrain is the descending part of the survey curve up to the break in the slope.
- The third terrain is the transition between the second and fourth terrains. These low resistivity values reflect the high electrical conductivity in this horizon.
- The fourth terrain is the ascending part of the curve with a slope of 45°. This particular rise reflects the presence of highly resistant crystalline rock at depth. However, there are drops in the apparent resistivity values, which show a gradual rise in apparent resistivity to form the 45° slope. These low apparent resistivity values are indicative of fractures and fissures at these depths, which represent water inflows (fracturing zone in sound rock).

4.7. Identification of aquifer zones on electrical surveys

Four to five aquifer zones were identified on the fourth (4th) survey curve (Table 3). The surveys directly above the "K" and "U" type anomalies each showed five (5) fracture points in the subsoil. Meanwhile, surveys conducted at points of "H"-type and "V"-type conductive anomalies showed four (4) fracture positions in the subsoil. These localized fractures represent the aquifer zones that will contribute to the productivity of the future catchment structure. Taking into account the number of fractures identified in the various electrical surveys, the "K" and "U" type conductive anomalies represent the first choice over the 'H' and "V" type conductive anomalies.

Table 3 Location of aquifer zones on the fourth plot of electrical survey curves

Electrical survey of conductive anomalies	Electrical drag	Identified fractures (FI)				
		FI 1	FI 2	FI 3	FI 4	FI 5
V	L0_0+00	24 - 36	50	70 -90	100 - 140	-
U	L0_0+00	24 - 28	32 - 40	55	70 - 90	130
K	L0_0+54 South	18 - 24	30 - 45	50 - 65	70 - 90	120 - 130
H	L0_1+00 North	20	45	60 - 80	100	-

4.8. Study of the cumulative length of fractures directly below identified conductive anomalies

Perpendicular to the identified conductive anomalies, the gross cumulative length of fractures intersecting a 4 ha grid (200 m x 200 m grid) varies from 420.37 m (type "H" anomaly) to 942.76 m (type "K" anomaly). Applying correction factors to the gross lengths, the corrected length values range from 362.92 m (type "H" anomaly) to 835.46 m (type "K" anomaly).

In order of high to low fracture density, analysis of the table shows that the type "K" anomaly (942.76 m for the gross length and 835.46 m for the corrected length) comes first, followed by the "U" type anomalies (556.26 m for the gross length and 496.02 m for the corrected length) and the "V" type (501.35 m for the gross length and 484.04 m for the corrected length) and finally the "H" type anomaly (420.37 m for the gross length and 362.92 m for the corrected length) comes last. Thus, for the study of the cumulative lengths of the fractures, the order of priority in the choice of the conductive anomaly is: K, U, V, and H (K > U > V > H).

Table 4 Gross and corrected lengths of fractures directly below the conductive anomalies

Conductive anomaly type	Priority fracture	Direction of fracture (°)	Gross fracture length (m)	Correction factor	Corrected fracture length (m)
U	Primary	238	236.29	1	236.29
	Secondary	230	187.67	0.99	185.84
	Secondary	298	107.25	0.5	53.62
	Secondary	202	25.05	0.81	20.27
	Total (m)		556.26		496.02
H	Primary	174	131.68	1	131.68
	Secondary	202	215.61	0.88	190.37
	Secondary	298	73.08	0.56	40.87
	Total (m)		420.37		362.92
V	Primary	230	260.88	1	260.88
	Secondaire	238	216.16	0.99	214.06
	Secondaire	298	24.31	0.37	9.11
	Total (m)		501.35		484.04
K	Primary	298	226.57	1	226.57
	Primary	238	236.29	1	236.29
	Secondary	174	118.48	0.44	51.94
	Secondary	202	205.45	0.81	166.21
	Secondary	230	155.97	0.99	154.45
	Total (m)		942.76		835.46

4.9. Summary of results and selection of the geophysical survey site

Analysis of the fracture index results, the number of fractures observed on the electrical sounding curves, and the lengths of the fractures directly below the V, U, K, and H conductive anomalies made it possible to propose a priority order for the selection of the drilling site. The summary of the results for the three parameters gave the following drilling order: K (F1) > U (F2) > V (F3) > H (F4).

Table 5 Summary of the ranks of the conductive anomalies and their drilling priority order

Conductive anomaly	Rank of conductive anomalies			Drilling priority order
	Fracture index (IF)	Fracture (aquifer zone)	Length of fractures	
V	2nd	2nd	3rd	F3
U	3rd	1st	2nd	F2
K	1st	1st	1st	F1
H	4th	2nd	4th	F4

4.10. Results at the end of drilling F1

Drilling F1 was carried out directly above the "K" type conductive anomaly, which showed the best results in terms of fracture index, number of fractures observed on its survey curve, and fracture length.

At the end of drilling, the technical data sheet for drilling F1 shows that a 13 m thick alteration zone was traversed before reaching sound rock, the depth of the drilled bedrock is 67 m, and the total depth of drilling F1 is 80 m. Three aquifer zones were identified in the bedrock, which facilitated the installation of 6 m (between 42 m and 48 m), 6 m (between 57 m and 63 m) and 9 m (between 69 m and 78 m) screened PVC pipes. A total of 21 m of screened PVC pipes were placed in the water catchment areas, resulting in a flow rate of 14 m^3/h.

Table 6 Characteristics of borehole F1 located directly above the "K" type anomaly

Weathering thickness (m)	**Total depth drilled (m)**	**Depth of drilled foundation (m)**	**PVC strainer 1**		**PVC strainer 2**		**PVC strainer 3**		**Flow rate (m^3/h)**
			Roof	Wall	Roof	Wall	Roof	Wall	
13	80	67	42	48	57	63	69	78	14

4.11. Comparative analysis of aquifers observed on the borehole curve and during drilling of F1

When comparing the number of aquifer zones identified on the borehole curve of anomaly K with that of borehole F1, it can be seen that only aquifers 2, 3, and 4 were observed during drilling of the catchment structure. In fact, the roofs and walls of aquifers 2, 3, and 4 of borehole F1 are included in those determined on the electrical survey curve of the "K" type conductive anomaly (Table 7).

Table 7 Comparison of aquifers identified on the K anomaly survey and in borehole F1

	Aquifer 1		**Aquifer 2**		**Aquifer 3**		**Aquifer 4**		**Aquifer 5**	
	Roof	Wall	Roof	Wall	Roof	Wall	Roof	Wall	Roof	Wall
Electrical survey of the K anomaly	18	24	30	45	50	65	70	90	120	130
Drilling F1	-	-	42	48	57	63	69	78	-	-
Result	No aquifer		Presence of aquifer		Presence of aquifer		Presence of aquifer		Depth not reached	

5. Discussion

The search for groundwater in crystalline rock environments relies primarily on locating fractures, as a borehole that does not cross any fractures cannot produce water [9]. It is therefore necessary to identify these geological discontinuities on a large scale using remote sensing. Satellite image processing has shown that the groundwater drainage structures in the study area are mainly oriented NW-SE (12.31%), N-S (10.77%), NE-SW (9.23%), NW-SE (9.23%) and NWW-SEE (9.23%). These directions were also confirmed by Kouakou et al. (2020), who also carried out work in the Kong region on groundwater resources. In order to intersect these NW-SE, N-S, NE-SW, NW-SE, and NWW-SEE fractures, the electrical profiles (electrical drags) were oriented in an east-west or west-east direction, which is the direction of the main fractures identified by processing Landsat 7 ETM+ images. According to [10], an electrical resistivity survey conducted in a direction oblique or perpendicular to the direction of the fractures can effectively detect groundwater reservoirs. In line with this horizontal prospecting approach, "H," "V," "K," and "U" type conductive anomalies were observed and positioned on fractures derived from Landsat 7 ETM+ image interpretation. In addition, the cumulative lengths of the fractures at which the identified conductive anomalies coincided showed a high fracture density in a 200 m x 200 m grid. This fracturing network in these grids made it possible to identify areas of intersection between fractures of different directions.

From a geophysical point of view, the conductive anomalies observed on the electrical profiles reflect areas of low resistivity similar to fractures in crystalline bedrock [11]. As a result, their fracture indices generally have values greater than 2 (FI > 2). These demonstrate that the subsoil of the study area has fractures with a high degree of fracturing.

According to [8] and [12], the fracturing index remains predominant when its value is greater than 2 (IF > 2). Indeed, these terrains are sometimes well fractured and therefore capable of containing a significant amount of water for drilling.

Electrical surveys were conducted directly above the H, K, H, and V conductive anomalies. Four (4) electrical fields were identified on the survey curves. The last field (the fourth deepest field) revealed the presence of four to five aquifer zones. From a hydrogeological perspective, these zones represent the locations of water inflows that contribute to the productivity of the boreholes. These findings corroborate the results of [10] in the Bounkani region, who asserts that it is the cumulative flow rate of each water inflow (aquifer zone) that determines the productivity of the borehole.

The combination of the results of the fracturing index, the lengths of the fractures from the Landsat 7 ETM+ images, and the number of aquifer zones identified on the electrical sounding curves prioritized the "K" type conductive anomaly for drilling. A comparison of the drilling results and electrical surveys showed that of the five (5) aquifer zones indirectly determined by the electrical resistivity method, only three (3) aquifer zones were actually observed during drilling. The disadvantage is that fractures are often observed on survey curves that are not present during drilling. However, the first aquifer zone was not identified during drilling. This may be due to the presence of wet or dry aquifers. These were also noted by [11] and [13], who believe that even if a fracture is detected during electrical sounding, it may correspond to a sterile fracture or a mineralized fracture with a very low water content. It should be noted that the last aquifer was not reached as it is located at a great depth. However, the three aquifer zones identified during drilling, located between 42 m and 78 m deep, were also observed on the survey curve of the "K" type conductive anomaly in the same depth range, resulting in a drilling position of 14 m^3/m, which meets the conditions for an HVA (Improved Village Hydraulics).

6. Conclusion

At the end of this study, combining data from the electrical resistivity method and remote sensing revealed important criteria for implementing a strategy to improve geophysical surveys. The directions of fractures (NW-SE, N-S, NE-SW, and NWW-SEE) derived from the interpretation of the Landsat 7 ETM+ satellite image showed that electrical trenches should be dug in an east-west (E-W) or west-east (W-E) direction in order to intersect as many fractures or fracture networks as possible. Thus, the east-west (E-W) oriented electrical profiles made it possible to locate four (4) conductive anomalies (V, U, K, and H) that coincided with the fractures identified from the ETM+ satellite image processing. The combination of fracture indices from electrical surveys, fracture lengths from remote sensing, and the number of aquifer zones seen on electrical sounding curves located directly above the conductive anomalies resulted in the following drilling priority order: K (F1) > U (F2) > V (F3) > H (F4). This led to the drilling of borehole F1, located at the same position as the "K" type conductive anomaly. In addition, borehole F1 has a depth of 80 m, with three aquifer zones that provided a high flow rate of 14 m3/h. This study therefore shows that the fracturing index, the length of the fractures, and the number of aquifer zones observed in the boreholes are criteria to be taken into account when deciding on the location of a geophysical site.

Compliance with ethical standards

Acknowledgements

This research was supported by the Hydrogeology and geophysics Research Group of the Geosciences and Environment Laboratory at Nangui Abrogoua University in Abidjan, Ivory Coast. The constructive and valuable comments of the anonymous readers and the Editor-in-Chief of the Journal are greatly appreciated.

Disclosure of conflict of interest

No conflict of interest to be disclosed.

References

[1] Loukou KGH., Kouakou KEG., Kouamé L. N., and Sombo BC. (2018). Prospection des eaux souterraines dans la localité de Bondoukou (Nord-est de la Côte d'Ivoire) : apport de la méthode électrique. Revue Ivoirienne des Sciences et Technologiques, 32, 172-187.

[2] Mangoua MJ., Kouassi KA., Douagui GA., Savané I., and Biémi J. (2019). Remote sensing and GIS contribution for groundwater mapping reservoirs in the Baya watershed (Eastern, region of Côte d'Ivoire). Journal of Geography, Environment and Earth Science International, 23 (3), 1-14.

[3] Kouakou KEG., Sombo AP., and Kéita D. (2020). Contribution de la télédétection et de la géophysique à l'implantation de forage d'eau à Kong, Nord-Est, Côte d'Ivoire. Afrique SCIENCE 16(1), 39-50.

[4] Lasm T., Gnamba F. M., Oga Y. M. S., Gnangne T., Biémi J. & Kouakou Y. K. N. (2014). Analyse de la productivité des aquifères de fissures du socle paléoprotérozoïque de la région de Katiola (Centre-Nord de la Côte d'Ivoire). European Scientific Journal, 10 (5), 79-98.

[5] Youan Ta M., Lasm T., Jourda JPR., Kouamé KF., and Razack M. (2008). Cartographie des accidents géologiques par imagerie satellitaire Landsat-7 ETM+ et analyse des réseaux de fractures du socle précambrien de la région de Bondoukou (Nord-Est de la Côte d'Ivoire). Télédétection, 8 (2), 119-135.

[6] Yésou H., Besnus Y., and Rolet J. (1993). Extraction of spectral information from Landsat TM data and merger with SPOT panchromatic imagery- a contribution to the study of geological structures. ISPRS Journal of Photogrammetry and Remote Sensing, 48 (5), 23-36. doi:10.1016/0924-2716(93)90069-Y

[7] Bouadou RAM., Kouassi KA., Kouassi FW., Coulibaly A., and Gnagne T. (2019). Use of the Inverse Slope Method for the Characterization of Geometry of Basement Aquifers: Case of the Department of Bouna (Ivory Coast). Journal of Geoscience and Environment Protection, 7, 166-183. https://doi.org/10.4236/gep.2019.76014

[8] Dieng B., Kouassi AH., and Bakyono BA. (2004). Optimisation des forages en zone de socle du Nord du Burkina Faso. Sud Sciences & Technologies, 12, 21-30.

[9] Kouadio KE., Savané I., Lasm T., and Biémi J. (2008). Hydrogeology prospecting in crystalline and metamorphic area by spatial analysis of productivity potential. European journal of scientific research, 22 (3), 373-390.

[10] Bouadou RAM. (2022). Couplage de la télédétection et la résistivité électrique dans l'identification des sites d'implantation de forages d'eau en milieu de socle fracturé dans la région du Bounkani (Nord-est de la Côte d'Ivoire). Thèse de Doctorat, Université NANGUI ABROGOUA, Abidjan, Côte d'Ivoire, 273 p.

[11] Kouassi Kouamé Auguste, Kouassi Francis Williams, Bouadou Rock Armand Michel, and Coulibaly Adama (2018). Comparative Study of Geophysical Prospection and Drilling Results in the Region of Gbêkê, Ivory Coast. Modern Environmental Science and Engineering, 4 (9), pp. 882-895.

[12] Kouakou K. E. G., Kouamé L. N., Sombo A. P., Djroh S. P., Sombo B. C. (2017). Résistivité électrique et géomorphologie : identification des aquifères de socle et critères pour le choix des points d'implantations des forages dans le département de Daoukro, Sud-Est Côte d'Ivoire. Afrique SCIENCE, 13 (3), pp. 98-112.

[13] Sombo, A. P. (2012). Application des méthodes de résistivités électriques dans la détermination et la caractérisation des aquifères de socle en Côte d'Ivoire. Cas des départements de Sikensi et de Tiassale (Sud de la Côte d'Ivoire). Thèse de Doctorat. Université Félix Houphouët Boigny de Cocody, Abidjan, Côte d'Ivoire, 203 p.

Appendix: Electrical survey curves

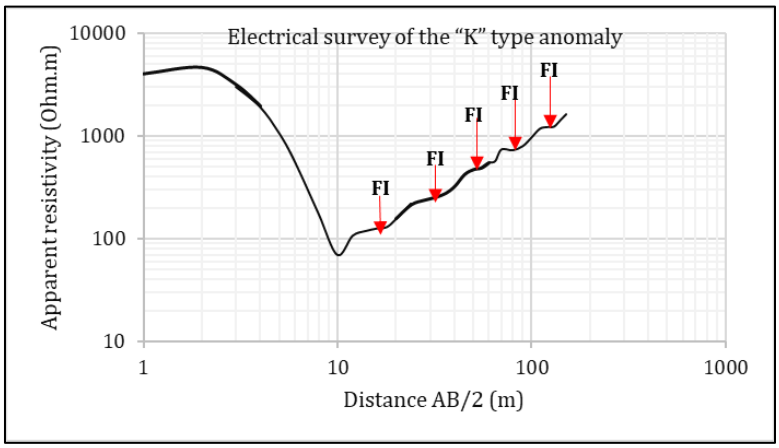

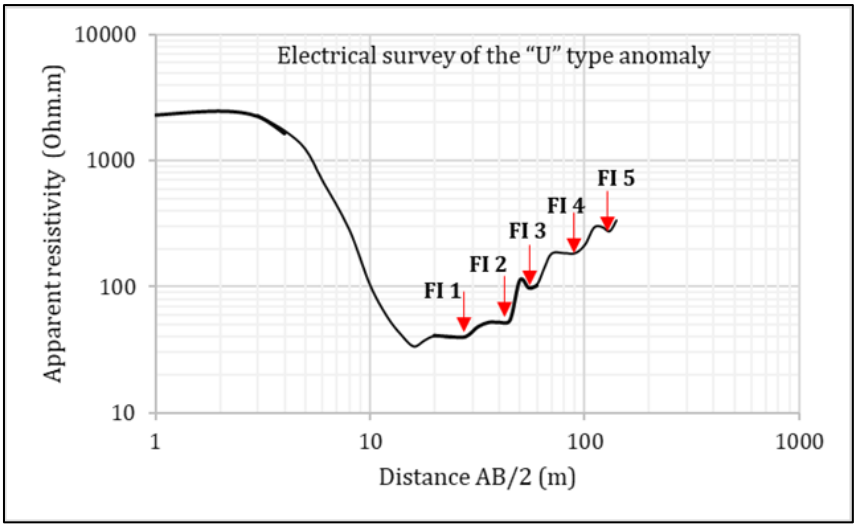
Electrical survey of the "U" type anomaly
Apparent resistivity (Ohm.m)
10000
1000
100
10
1
10
100
1000
Distance AB/2 (m)
FI 1
FI 2
FI 3
FI 4
FI 5

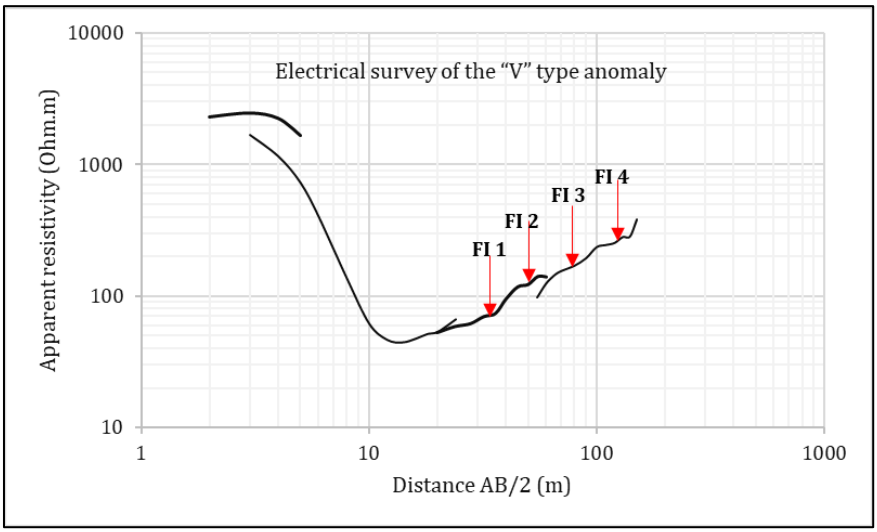
Electrical survey of the "V" type anomaly
Apparent resistivity (Ohm.m)
10000
1000
100
10
1
10
100
1000
Distance AB/2 (m)
FI 1
FI 2
FI 3
FI 4

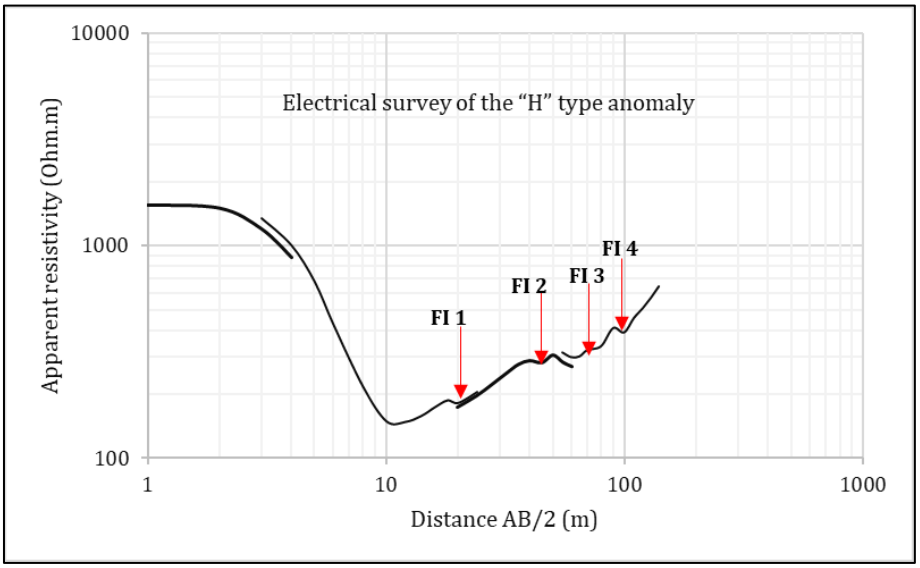
Electrical survey of the "H" type anomaly
Apparent resistivity (Ohm.m)
10000
1000
100
1
10
100
1000
Distance AB/2 (m)
FI 1
FI 2
FI 3
FI 4